Aspects of Molecular Medicine 5 (2025) 100074

Contents lists available at ScienceDirect

Aspects of Molecular Medicine

journal homepage: www.journals.elsevier.com/aspects-of-molecular-medicine

Unveiling potential antiviral phytochemicals from *Molineria capitulata* (Lour.) Herb. against varicella-zoster virus: Ethnomedicinal insights and computational analysis

Md. Nur Kabidul Azam [a,c,*], Md Nasir Ahmed [b,c,**], Partha Biswas [a], Amia Kandker [c], Md. Mohaimenul Islam Tareq [a], Labib Shahriar Siam [a], Md. Nazmul Hasan [a]

[a] *Laboratory of Pharmaceutical Biotechnology and Bioinformatics, Department of Genetic Engineering and Biotechnology, Jashore University of Science and Technology, Jashore, Bangladesh*
[b] *Department of Biotechnology and Genetic Engineering, University of Development Alternative, Dhaka, Bangladesh*
[c] *Biotechnology and Natural Medicine Division, TechB Nutrigenomics, Dhaka, Bangladesh*

ARTICLE INFO

Handling Editor: Prof A Angelo Azzi

Keywords:
Plant-based antivirals
Computational drug development
Ethno-phytomedicine
Curculigo

ABSTRACT

Varicella-Zoster Virus (VZV), causing chickenpox and potentially severe later-life complications, is traditionally treated by the Musahar tribe in Bangladesh using *Molineria capitulata* in a polyherbal formulation. This plant is also recognized in other regions for its anti-infective properties. This study aimed to evaluate the ethnomedicinal efficacy of *Molineria capitulata* against VZV using computational drug development approaches and to review its traditional medicinal uses. An ethnomedicinal survey was conducted, followed by QSAR, molecular docking, molecular dynamics simulation, ADMET and MM-GBSA analysis to assess potential treatments for VZV. Literature searches on PubMed and Google Scholar provided additional insights into the traditional antimicrobial uses of the plant. Twenty-four phytochemicals were screened against VZV thymidine kinase, revealing three with significant binding affinity (less than −10 kcal/mol): capituloside, curcapital, and pilosidine. These compounds showed strong protein interactions and stability in 100 ns simulations. Pilosidine had the highest docking score (−12.471 kcal/mol), followed by capituloside (−12.213 kcal/mol) and curcapital (−11.360 kcal/mol). Valacyclovir, the control, had a lower score (−5.807 kcal/mol). Pharmacokinetic profiles and QSAR analysis indicated their potential as lead compounds. Capituloside and pilosidine were effective against Herpes, Influenza, and Hepatitis B, while curcapital was effective against CMV, Herpes, Influenza, and Adenovirus. The physicochemical properties of these compounds highlight their significant potential as antiviral agents. The MM-GBSA evaluation indicated that among the complexes, the pilosidine-protein complex had the greatest free binding energy, with a value of −67.15 kcal/mol. *Molineria capitulata* holds promise for antiviral therapy development, and validating the therapeutic potential of capituloside, curcapital, and pilosidine against varicella-zoster virus requires comprehensive in-vitro and in-vivo studies.

1. Introduction

1.1. Varicella-zoster virus: Pathogenesis and treatment challenges

The Varicella-zoster virus (VZV) is a highly contagious human virus with a double-stranded DNA genome, belonging to the herpesvirus's family of α-herpesviruses (Gershon et al., 2015; Pergam and Limaye, 2009). VZV is prevalent worldwide and causes two main infections: varicella (chickenpox) and herpes zoster (shingles). VZV can trigger antibodies (IgG, IgM, and IgA) that bind to viral proteins and infect T lymphocytes, epithelial cells, and ganglia (Arvin, 1996; Gershon et al., 2015).

Varicella (chickenpox) manifests as an itchy and blistering rash with small red spots that cover the entire body. It can be life-threatening in immunosuppressed patients, potentially leading to damage to the central nervous system (Freer and Pistello, 2018). After the initial infection,

* Corresponding author. Laboratory of Pharmaceutical Biotechnology and Bioinformatics, Department of Genetic Engineering and Biotechnology, Jashore University of Science and Technology, Jashore, Bangladesh.
** Corresponding author. Department of Biotechnology and Genetic Engineering, University of Development Alternative, Dhaka, Bangladesh.
E-mail addresses: azam10bt@gmail.com (Md.N.K. Azam), nasir.ahmedbd@hotmail.com (M.N. Ahmed).

https://doi.org/10.1016/j.amolm.2025.100074
Received 7 December 2024; Received in revised form 2 March 2025; Accepted 4 March 2025
Available online 19 March 2025

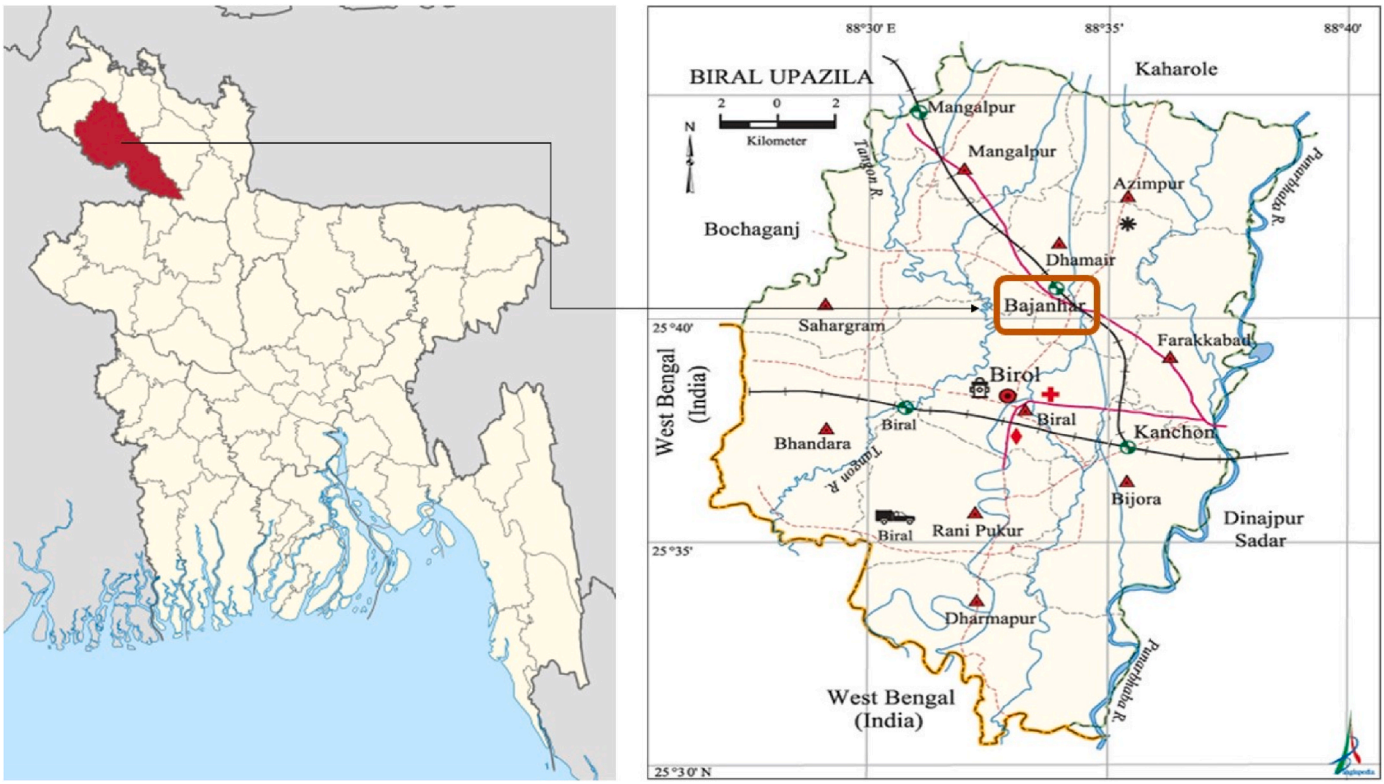

Fig. 1. Map of the location of surveyed area, Bajanhar, Biral subdistrict, Dinajpur, Bangladesh (Map source: Banglapedia [https://en.banglapedia.org/index.php/Biral_Upazila]).

VZV can remain dormant in the ganglia (Gershon et al., 2015; Pergam and Limaye, 2009) and later reactivate as zosters (shingles) (Gershon, 2017). The pathophysiology and mechanism by which VZV is transferred from lymphocytes to nerve cells and its dormancy remain unexplored (Gershon et al., 2015).

Decades after becoming latent, the virus can reactivate, triggered by several factors (Depledge et al., 2018; Eshleman et al., 2011; Kennedy et al., 2021). The disease is more severe among immunosuppressed individuals, leading to post-herpetic and neurological disorders such as vasculitis (Kennedy and Gershon, 2018). Although vaccination is available, limited resources, costs, health insurance policies, and storage requirements mean that not everyone can be vaccinated (Komara, 2009). Therefore, VZV infection continues to pose threats, particularly for the elderly and immunosuppressed, even in the post-vaccine era. In addition to vaccination, antiviral drugs such as Acyclovir are used, but come with adverse side effects, including headaches, vomiting, renal dysfunction, and neurotoxic effects (Sauerbrei, 2016, 2016a).

1.2. Molineria capitulata: bridging ethnomedicine and contemporary antiviral research

Plant-based ethnomedicinal knowledge or traditional medicine is a great resource for the development of new biomedicines, as plants contain enormous bioactive compounds with extensive pharmacological attributes and drug-like properties (Yuan et al., 2016). From 1960 to 2019, over 110,000 medicinal plant-based studies were published worldwide (Salmerón-Manzano et al., 2020). Medicinal plants or phytomedicines have been used as natural remedies since ancient times and are considered the origin of modern drug discovery (Fitzgerald et al., 2020). Isolated antiviral bioactive compounds from plants can target specific phases of the viral life cycle, enhance protein function, and inhibit viral entry and assembly, blocking viral replication, viral enzymes, and membrane proteins. Recent advances in in-vitro studies have revealed a plenitude of promising antiviral phytochemicals (Ahmed and Hughes, 2022; de Castro Barbosa et al., 2022; Owen et al., 2022).

Bangladesh has over 100 indigenous communities rich in traditional medicinal knowledge, relying mainly on medicinal plants. The Musahar community is among the most vulnerable tribal communities in Bangladesh, living in the Dinajpur and Habiganj districts. Apart from Bangla, they speak Musha or Napali (of Hindi origin) and adhere to Hindu mythology (Islam and Parvez, 2013). The authors conducted an ethno-medicinal plant survey among the Musahar tribal community that resides in the Dinajpur district, Bangladesh, documenting the use of *Molineria capitulata*, synonym *Curculigo capitulata* (Lour.) Kuntze (family Hypoxidaceae) against chickenpox.

This present article is an effort to present in-silico evaluations, particularly QSAR, molecular docking, molecular dynamic simulations, and ADMET analysis of the traditionally used medicinal plant, *Molineria capitulata*, for the treatment of chickenpox by folk medicine practitioners of the Musahar tribal community residing in Bangladesh. Our aim was to investigate the antiviral properties of *Molineria capitulata* to address the need for alternative chickenpox treatments without adverse side effects, and to expand our understanding of the vast applications of phytochemicals as medicine by combining traditional wisdom with modern scientific methodologies.

2. Methods and materials

2.1. Survey area and plant data collection

An ethnomedicinal plant survey was conducted between March 2018 and August 2018 in the northern part of the Biral subdistrict, near Dhukur-jhari in the Gobindapur union in Bajanhar, Dinajpur district, Bangladesh. During the survey, two tribal healers from the Musahar community, Keshob Musahar and Atul Musahar, were interviewed to collect ethnomedicinal information on the various plants they used against various diseases. After collecting plant specimens, the samples were submitted to the National Herbarium for identification, where

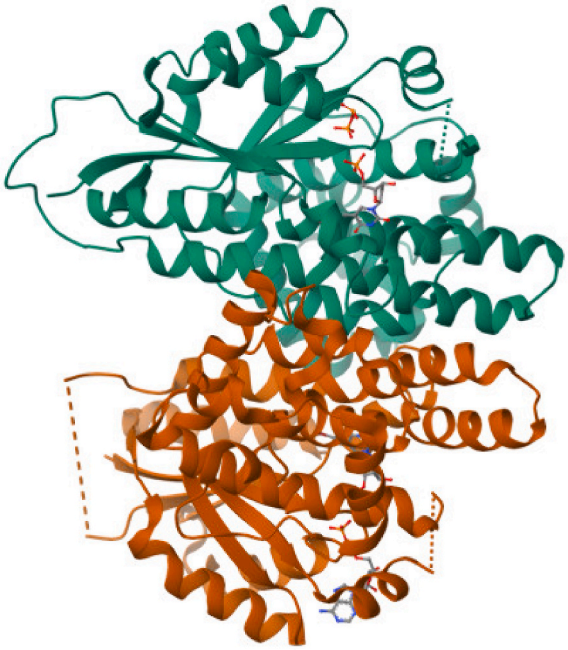

Fig. 2. Three-Dimensional structure of selected protein.

Fig. 3. The leaf of *Molineria capitulata* (Lour.) Herb.

Molineria capitulata (Lour.) Herb., locally called 'Agun Kumari', was assigned the accession number DACB 85913. Fig. 1 shows the map of the survey location.

2.2. Literature search

The literature search was conducted in PubMed and Google Scholar databases with the following keywords: "*Molineria capitulata* ethnomedicine ethnobotany"; "*Molineria capitulata* pharmacology"; "*Molineria capitulata* phytochemicals bioactive compounds"; "ethnobotanical *Molineria capitulata*"; "*Molineria capitulata* antimicrobial activity" etc. for the accumulation of ethnomedicinal usage against infections reported from other geographical locations, and antimicrobial efficacy information.

Table 1
Antiviral activity of four selected phytocompounds using QSAR analysis.

SN	CID (Phytocompound)	Pa	Pi	Activity
1	3013844 (Capituloside)	0.489	0.011	Antiviral (Herpes)
		0.310	0.033	Antiviral
		0.331	0.072	Antiviral (Influenza)
		0.272	0.042	Antiviral (Hepatitis B)
2	10096608 (Pilosidine)	0.489	0.011	Antiviral (Herpes)
		0.310	0.033	Antiviral
		0.331	0.072	Antiviral (Influenza)
		0.272	0.042	Antiviral (Hepatitis B)
3	10733722 (Curcapital)	0.366	0.052	Antiviral (Herpes)
		0.267	0.114	Antiviral (Influenza)
		0,254	0,134	Antiviral (Adenovirus)
		0.819	0.001	Antiviral (CMV)
4	135398742 (Valacyclovir as a control)	0.801	0.004	Antiviral
		0.760	0.007	Antiviral (Poxvirus)
		0.705	0.003	Antiviral (Herpes)

Table 2
Compound CIDs, chemical formulas, and binding scores of top four ligands and control drug with thymidine kinase protein.

Ligands for thymidine kinase protein (PDB ID: 1OSN)				
Ligands PubChem CID Number	Compounds Name	Docking Score (kcal/mol)	Amino Acid Involved Interaction	
			Hydrogen Bond Interaction	Hydrophobic Bond Interaction
10096608	Pilosidine	−12.471	Gln90 – 2.76 Å Gln90 – 2.94 Å Thr26 – 2.64 Å Arg54 – 2.94 Å	Tyr66, Ser135, Ile65, Ile62, Glu192, Tyr21, Leu50, Glu48, Phe139, Phe93
3013844	Capituloside	−12.213	Glu192 – 2.73 Å Lys25 – 3.28 Å Gly22 – 2.87 Å Arg130 – 2.91 Å Tyr66 – 2.80 Å	Tyr21, Leu50, Ile62, Thr26, Glu48, Ala134, Phe93, Phe139, Ser135, Trp53
10733722	Curcapital	−11.360	Glu48 – 2.58 Å Arg143 – 2.70 Å Gln90 – 2.53 Å	Arg130, His97, Ala134, Trp53, Phe93, Phe139, Ile65, Tyr66, Tyr21
135398742 (Control)	Valacyclovir	−5.807	Thr26 – 2.80 Å Thr26 – 3.19 Å Gly22 – 2.95 Å	Glu48, Ile62, Trp53, Phe93, Tyr21, Phe139, Gln90, Ser135, Ala134, Arg130, Lys25

2.3. In-silico evaluation

2.3.1. Protein selection and preparation

Key molecular targets for chickenpox include thymidine kinase (TK), which is crucial for VZV replication. TK, a phosphotransferase enzyme, catalyses the transfer of phosphate groups from ATP to deoxythymidine, forming deoxythymidine monophosphate. This protein, encoded by VZV, possesses both thymidine and thymidylate phosphorylating

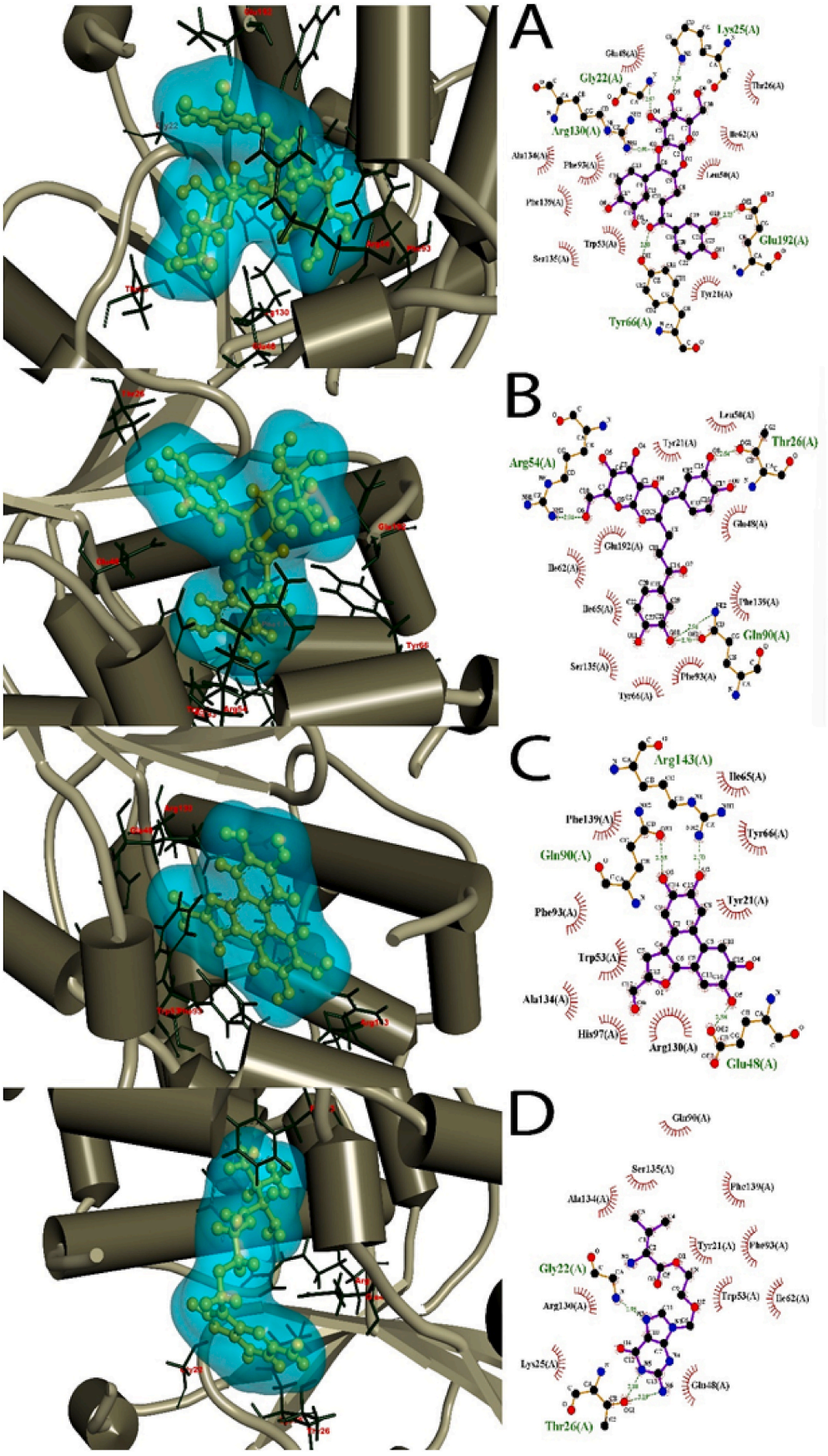

(caption on next page)

Fig. 4. The interactions between selected phytocompounds and the thymidine kinase protein. The figure is divided into two parts: on the left, the three-dimensional complexes of protein-ligand interactions are shown, while on the right, the two-dimensional representations are provided. The interactions are detailed as follows: (A) capituloside - thymidine kinase protein, (B) pilosidine - thymidine kinase protein, (C) curcapital - thymidine kinase protein, (D) valacyclovir - thymidine kinase protein. This layout provides a comprehensive view of both the spatial and planar interactions between the ligands and the target protein.

Table 3
ADMET profiling of the physicochemical and pharmacological properties of the phytocompounds and control drug.

Physicochemical									Pharmacological						
Ligands	MW	HAc	HD	NRB	MoR	SA	NLV	DL	IA	BBB	TC	AT	LD50	HT	MDT
CID 3013844 Capituloside	478.45 g/mol	11	7	6	114.99	186.37	2	Yes	45.731	No	0.105	No	2.665	No	0.234
CID 10096608 Pilosidine	478.45 g/mol	11	7	6	114.99	186.37	2	Yes	45.731	No	0.105	No	2.665	No	0.234
CID 10733722 Curcapital	310.26 g/mol	6	4	1	84.71	111.13	0	Yes	85.464	No	0.191	Yes	2.491	No	0.53
CID 135398742 Valacyclovir	324.34 g/mol	7	3	8	82.54	151.14	0	Yes	45.932	No	0.852	No	2.282	Yes	0.551

*ADMET: absorption, distribution, metabolism, excretion, and toxicity; MW: molecular weight; HAc: No. of hydrogen bond acceptor; HD: No. of hydrogen bond donor; NRB: No. of rotatable bonds; IA: intestinal absorption; TC: total clearance, log mL/(min·kg); LD50: oral rat acute toxicity, mg/kg; BBB: blood-brain barrier; HT: hepatotoxicity; AT: AMES toxicity; MTD: maximum tolerated dose for a human, log mg/(kg·day); NLV: No. of Lipinski's rule violations; DL: drug-likeness.

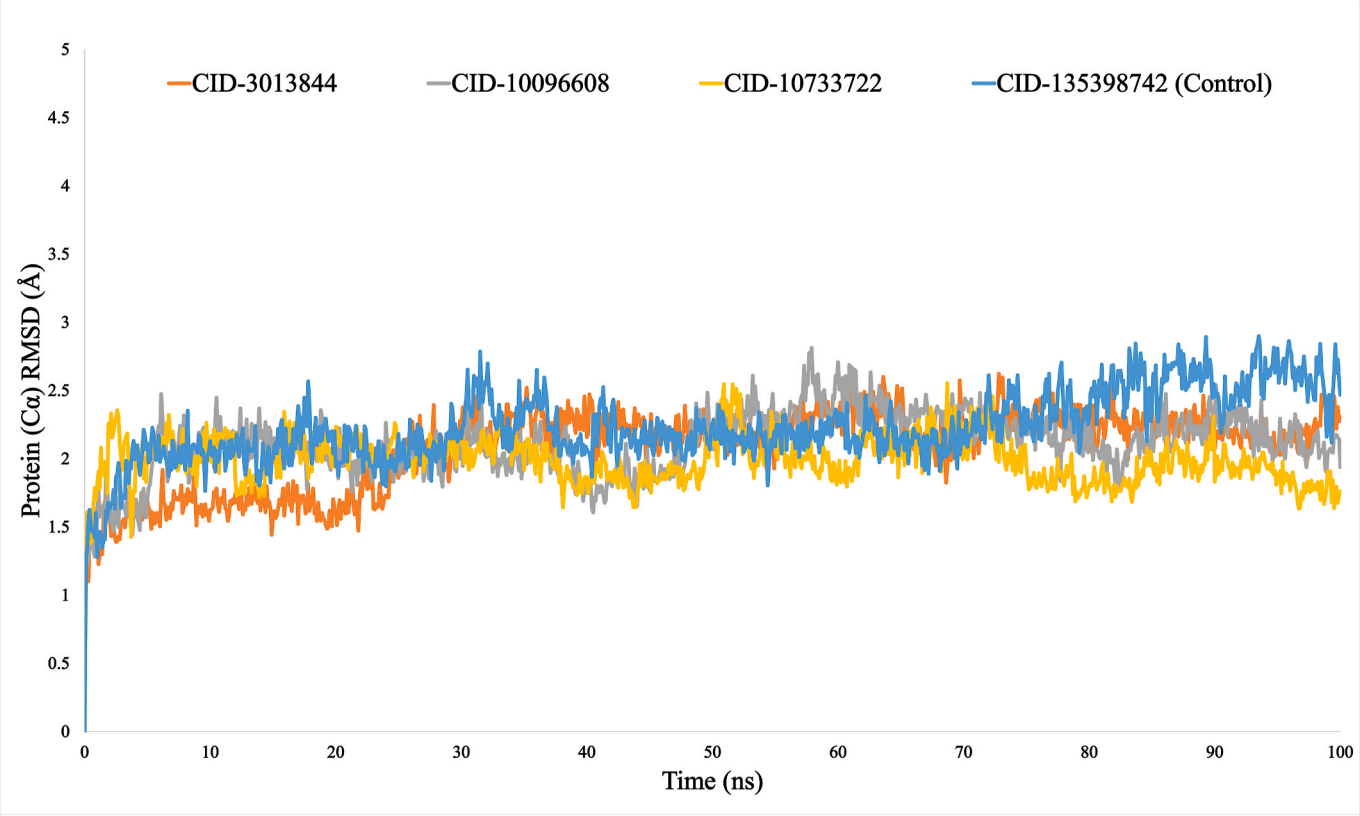

Fig. 5. The RMSD values for the thymidine kinase protein (PDB: 1OSN) in complex with four ligand compounds, derived from the Cα atoms of the system, are depicted in the figure. The selected compounds capituloside (CID: 3013844), pilosidine (CID: 10096608), curcapital (CID: 10733722), and Valacyclovir (CID: 135398742) as control, are represented by red, violet, yellow, and blue colours, respectively. (For interpretation of the references to colour in this figure legend, the reader is referred to the Web version of this article.)

activities, essential for viral DNA replication (Kwofie et al., 2022). The crystallographic X-ray coordinates of this TK protein complexed with BVDU-MP and ADP, with a resolution of 3.20 Å, are available under the accession code 1OSN from the Protein Data Bank (PDB), see Fig. 2. The selected protein's crystal structures were initially optimized using the Protein Preparation Wizard module in Schrödinger software. This optimization process involved removing bound ligands and water molecules, eliminating alternate amino acid conformations, adding missing atoms and polar hydrogens, and assigning Kollman charges to ensure complete charge assignment.

2.3.2. Ligand activity prediction by QSAR analysis

Several bioactive phytochemical compounds from *Molineria capitulata* have been documented in previous studies, although not all of their chemical structures were identified. The chemical structures of 24 bioactive phytochemicals were recovered from the PubChem database.

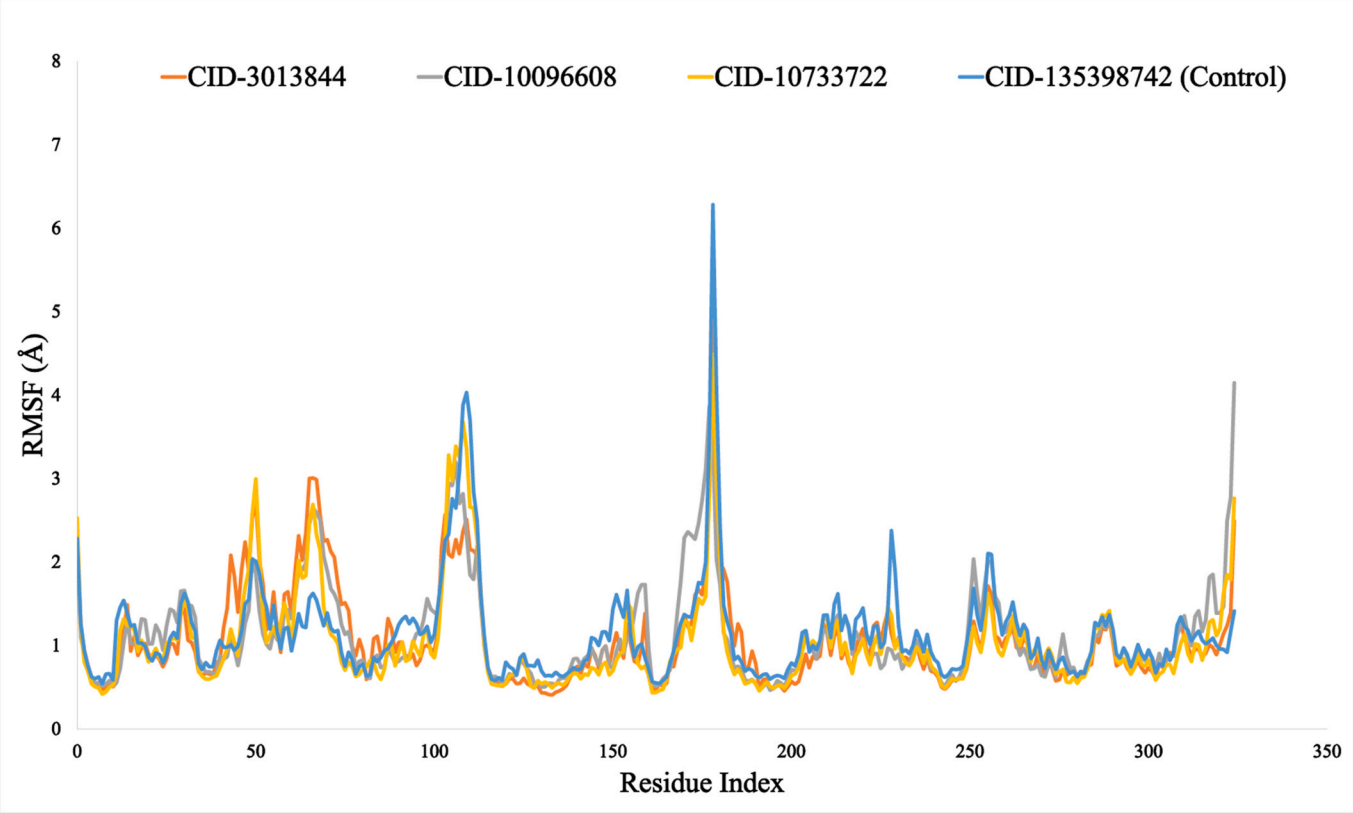

Fig. 6. RMSF values for the thymidine kinase protein model in complex with four ligand compounds, derived from the Cα atoms of the system, are depicted in the graph. The selected compounds, capituloside (CID: 3013844), pilosidine (CID: 10096608), curcapital (CID: 10733722), and Valacyclovir (CID: 135398742) as control, are represented by red, violet, yellow, and blue colours, respectively. (For interpretation of the references to colour in this figure legend, the reader is referred to the Web version of this article.)

These compounds include 1-*O*-methylcurculigine, 1-*O*-methyl isocurculigine, 2-4-dichloro-5-methoxy-3-methyl phenol, 2-6-dimethoxy benzoic acid, 3-4-dihydroxy benzoic acid ethyl ester, 3-4-hydroxy-3-methoxyphenylacryl aldehyde, 4-ethoxy-3-hydroxymethyl phenol, 4-hydroxybenzaldehyde, Breviscapin B, Breviscaside A, Breviscaside B, Capituloside, Crassifogenin C, Crassifoside A, Crassifoside D, Crassifoside F, Curcapital, Curcapitoside, Curculigine, Curlignan, Daucosterol, Iscurculigine, Pilosidine, and Orcinol glucoside (Nie et al., 2013; Shovo et al., 2021).

The biological activities of these 24 phytochemicals were evaluated using the PASS (Prediction of Activity Spectra for Substances) server (http://www.way2drug.com/passonline). This server predicts the biological activity of substances based on their structural makeup using the Structure-Activity Relationship Base (SAR Base). The SMILES format of the phytochemicals was inputted into the server, which calculated the probability that each compound was active (Pa) or inactive (Pi). Only activities specifically relevant to antiviral properties were considered.

2.3.3. Ligand preparation

The ligand structures were prepared using the LigPrep module in the Maestro application, part of the Schrödinger Suite Software (https://www.schrodinger.com/products/maestro). The minimisation process utilised the OPLS3e force field in conjunction with the Epik ionizer, typically operating within a pH range of 7.0 ± 2.0. This approach generates up to 32 conformers per structure, maintaining an RMSD threshold of 1.0 Å. The Epik ionizer helps to accurately predict the protonation states of the ligands, which is crucial for reliable docking results. This comprehensive preparation ensures that the ligands are in their most stable and biologically relevant conformations before proceeding to further computational analyses (Johnston et al., 2023).

2.3.4. Molecular docking

In Maestro version 11.5, the Glide tool was utilised for docking studies. Initially, a prepared library of ligands (phytochemicals) was docked into the active site of the target protein (1OSN) using the standard precision (SP) mode, which allowed for variable ligand sampling (David et al., 2018). This was followed by extra precision (XP) docking, where ligand sampling was turned off with the setting 'no refine only'. The initial docking analysis was performed on the co-crystallized ligand to assess its binding affinity at the active site of the target protein before proceeding with the docking of the compound libraries.

2.3.5. Post docking data Visualization

After the docking process was completed, the top-ranking conformations were selected for a detailed analysis of protein-ligand interactions. These interactions were visualized in both two-dimensional and three-dimensional formats using LigPlot + v.2.2 and BIOVIA Discovery Studio Visualizer 2021, respectively (Srivastava et al., 2021, 2022).

2.3.6. Pharmacokinetic and toxicity profiling of the potential ligands

The pharmacokinetic properties of the potential phytochemicals were predicted using the ADMETlab, pkCSM, and SwissADME web tools (Daina et al., 2017; Pires et al., 2015; Xiong et al., 2021). These tools accurately predict pharmacokinetic parameters, including the physicochemical properties, absorption, distribution, metabolism, and excretion (ADME) of the compounds. The drug likeness was evaluated using Lipinski's rule of five. Furthermore, the toxicity profiles of the compounds were predicted using ProTox-II, which provides comprehensive toxicity information (Banerjee et al., 2018; Bitew et al., 2021).

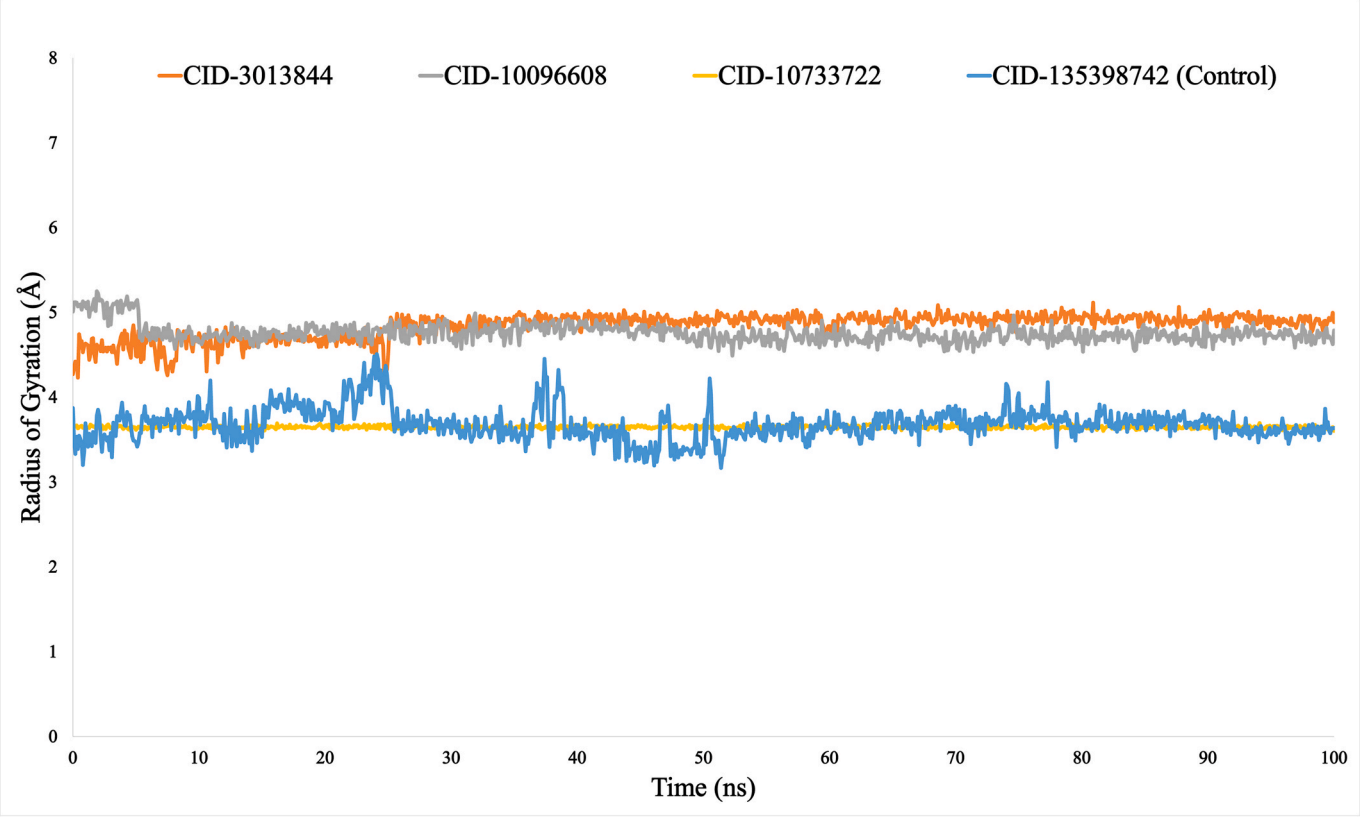

Fig. 7. A 100 ns simulation was conducted to determine the radius of gyration (Rg) of the protein-ligand interactions. The selected compounds, capituloside (CID: 3013844), pilosidine (CID: 10096608), curcapital (CID: 10733722), and Valacyclovir (CID: 135398742) as control, are represented by red, violet, yellow, and blue colours, respectively, in complex with the protein. (For interpretation of the references to colour in this figure legend, the reader is referred to the Web version of this article.)

2.3.7. Molecular dynamic (MD) simulation and Prime MM-GBSA calculation

We conducted 100 ns MD simulations to evaluate the stability of selected ligands: capituloside (CID: 3013844), pilosidine (CID: 10096608), curcapital (CID: 10733722), and valacyclovir (CID: 135398742) as a control, binding to the thymidine kinase protein model. Utilizing Desmond v3.6 in Schrödinger on a Linux machine, we simulated the protein-ligand complexes to assess their thermodynamic stability. A Transferable Intermolecular Potential with 3 Points (TIP3P) water model was employed to maintain a specified volume within an orthorhombic periodic bounding box shape, separated by 10 Å. The solvent system was neutralized with $Na+$ and Cl^- ions. The system was then minimized and relaxed using Optimized Potentials for Liquid Simulations 3 Enhanced (OPLS3e) force field constants.

Equilibration was carried out in two stages: first in an NVT ensemble using the Berendsen temperature-coupling method, followed by a Number of particles (N), Pressure (P), and Temperature (T) (NPT) ensemble at 300 K and 1 atm using the Parrinello-Rahman barostat method. The MD simulations were conducted for 100 ns under constant pressure. Maestro in Schrödinger was used to create all MD simulation screenshots. The quality of the MD simulation was verified using the simulation interaction diagram (SID) of the Desmond modules in the Schrödinger suite.

We assessed stability using various metrics such as RMSD (Root Mean Square Deviation), RMSF (Root Mean Square Fluctuation), protein-ligand contacts, intramolecular hydrogen bonds, SASA (Solvent Accessible Surface Area) values, radius of gyration (Rg), MolSA (Molecular Surface Areas), protein-ligand interactions, and PSAs (Polar Surface Areas). RMSD measures the average distance between an atom's position at a specific time and its reference position, while RMSF tracks local changes in the conformational structure of the protein complex.

Additionally, the estimation of free energy changes for ligand-receptor complexes was conducted following the docking process. The analysis utilised the Schrödinger Maestro MM-GBSA module, which is designed for calculating binding free energies based on molecular mechanics and generalized Born surface area methods.

3. Results

3.1. Molineria capitulata: traditional formulations by Musahar healers and global anti-infective uses

The Musahar tribal healer prepares a lotion by combining the juice of *Molineria capitulata* leaves (Fig. 3) with mustard (*Brassica juncea*) oil, *Piper nigrum* (black pepper), and cinnabar (mercuric sulphide, HgS). This lotion is then applied to the skin infected with chickenpox. Additionally, reviews of the literature reveal that *Molineria capitulata* is used in traditional medicine in various countries to treat multiple infections. For example, the Khiamniungan and Naga tribes of India use it to treat eye infections (conjunctivitis) (Changkija, 1999; Kichu et al., 2015; Ozukum et al., 2019), while traditional Dai medicine uses it for urinary tract infections and gonorrhea (Nie et al., 2013). The Dayak Tomun tribes of Indonesia use it to alleviate itching (Santoso et al., 2019). Furthermore, the leaves of *Molineria capitulata* are used by the Apatani tribe in India to reduce infections in the preparation of herbal black salt, combined with *Ambrosia artemisiifolia* (Panda et al., 2016).

The fruits of *Molineria capitulata* serve as an alternative food source for the Temiar tribal people of Malaysia during the monsoon flood season (Ayob et al., 2016). The rootstock is cooked and consumed as a vegetable by the Naga tribes in India (Kichu et al., 2015). Furthermore,

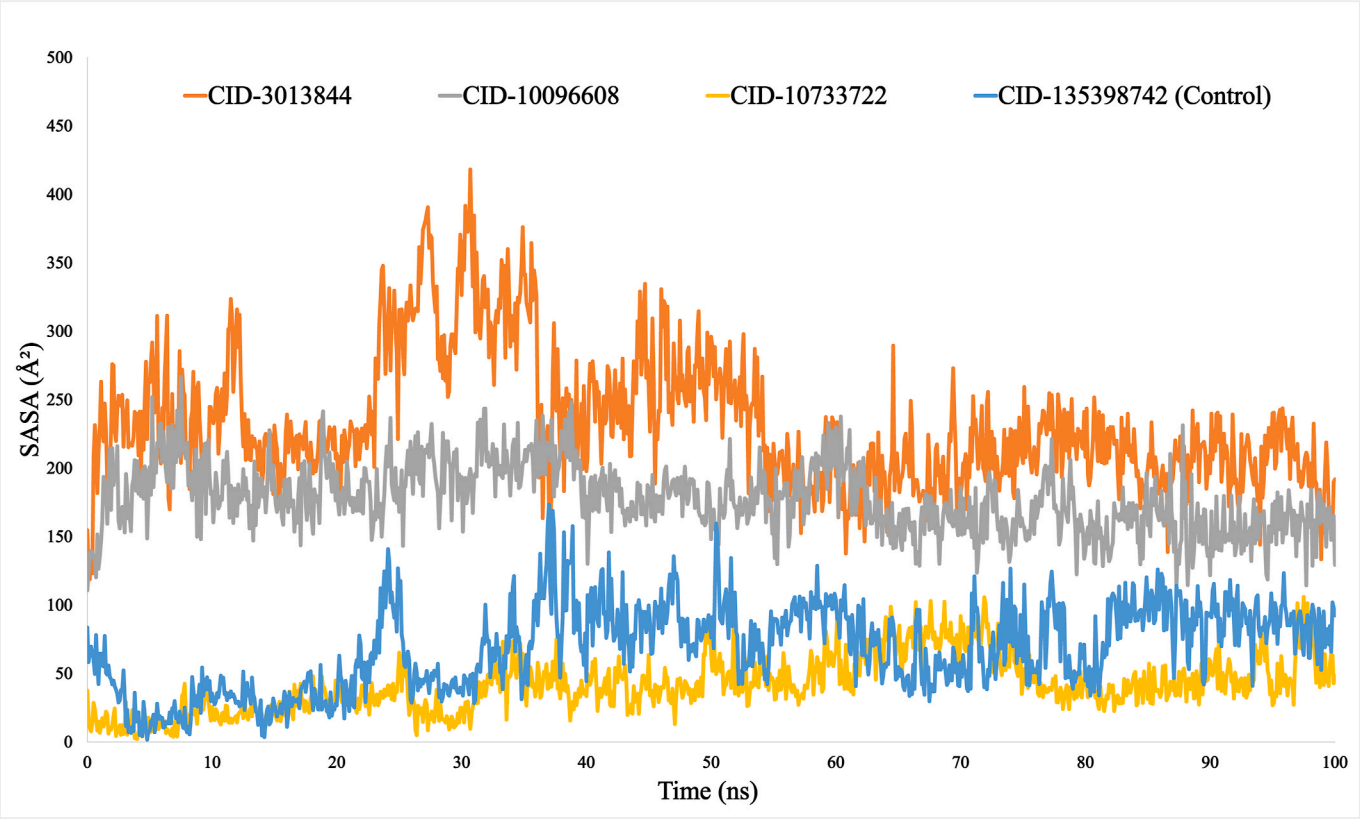

Fig. 8. The solvent accessible surface area (SASA) of the protein-ligand interaction compounds was calculated from the 100 ns simulation interaction diagram. The selected compounds capituloside (CID: 3013844), pilosidine (CID: 10096608), curcapital (CID: 10733722), and Valacyclovir (CID: 135398742) as control, are represented by red, violet, yellow, and blue colours, respectively, in complex with the protein. (For interpretation of the references to colour in this figure legend, the reader is referred to the Web version of this article.)

fruit is a staple diet for the Monpa (Li et al., 2020) and Lhoba (Yang et al., 2020) communities in Medog County, Tibet, China. In particular, *Molineria capitulata fruit* has a higher calcium content compared to guava, along with a good amount of vitamin C and a low glucose level (Briliani et al., 2018).

3.2. Antimicrobial efficacy of Molineria capitulata

Essential oils extracted from *Molineria capitulata* fruits, together with isolated myrcene, have demonstrated significant antimicrobial activity against pathogens such as *Staphylococcus aureus, Escherichia coli, Salmonella typhi, Pseudomonas aeruginosa, Klebsiella pneumoniae, Fusarium oxysporum* and *Neisseria gonorrhoeae* (Umaru et al., 2020). Additionally, a newly isolated *Streptomyces* sp. 5–10 of the plant roots has shown promising antifungal activity against *Fusarium oxysporum* (Yun et al., 2021). Furthermore, the rhizomes of *M. capitulata* contain chlorine-containing phenoloid, specifically capitulatin A and nyasicoside, which can act as natural surfactants (Dembitsky, 2005).

3.3. QSAR (Quantitative structure-activity relationship) analysis

We evaluated 24 phytocompounds for their potential to suppress viral infections, specifically chickenpox, using PASS online software (http://www.way2drug.com/passonline). On the basis of their combined antiviral effects, we selected four phytocompounds, including a control drug. Compounds with higher Pa (probability of activity) values are considered to have greater medicinal potential and experimental value. From our QSAR model research, we identified the top four phytocompounds using a Pa cut-off value of >250 (Table 1). Although PASS cannot predict the binding affinity for new therapeutic targets, it helps to identify drugs with fewer unwanted effects. The four selected phytocompounds were then subjected to site-specific supramolecular docking and an assessment of the ADMET property for further analysis.

Capituloside and pilosidine exhibit significant antiviral activities, particularly against Herpes, with Pa values of 0.489 and Pi values of 0.011, along with moderate efficacy against general antiviral, Influenza, and Hepatitis B viruses. Curcapital shows notable antiviral activity, especially against *Cytomegalovirus* (CMV), with a Pa value of 0.819 and a Pi value of 0.001, and also exhibits activity against Herpes, Influenza, and Adenovirus. Valacyclovir, used as a control, demonstrates a broad-spectrum antiviral effect, with high efficacy against Poxvirus and Herpes, confirmed by Pa and Pi values of 0.801 and 0.004, respectively. These insights underscore the potential of capituloside, pilosidine, and curcapital as promising antiviral agents, encouraging further in-vitro and in-vivo studies to validate their efficacy. The use of Valacyclovir as a control reinforces the reliability of these phytocompounds' antiviral properties.

3.4. Molecular docking

To investigate the inhibition affinity of selected bioactive phytochemicals, molecular docking was conducted to identify their optimal conformations and interactions with the active sites of target proteins, with the aim of developing potential drugs against chickenpox. Initially, virtual screening of the phytochemicals against the selected proteins yielded multiple conformations. However, we focused only on interactions with a binding affinity of −10 kcal/mol or lower, which revealed that thymidine kinase proteins interacted with all ligands (Table 2).

The key findings from the binding affinities of the ligands for

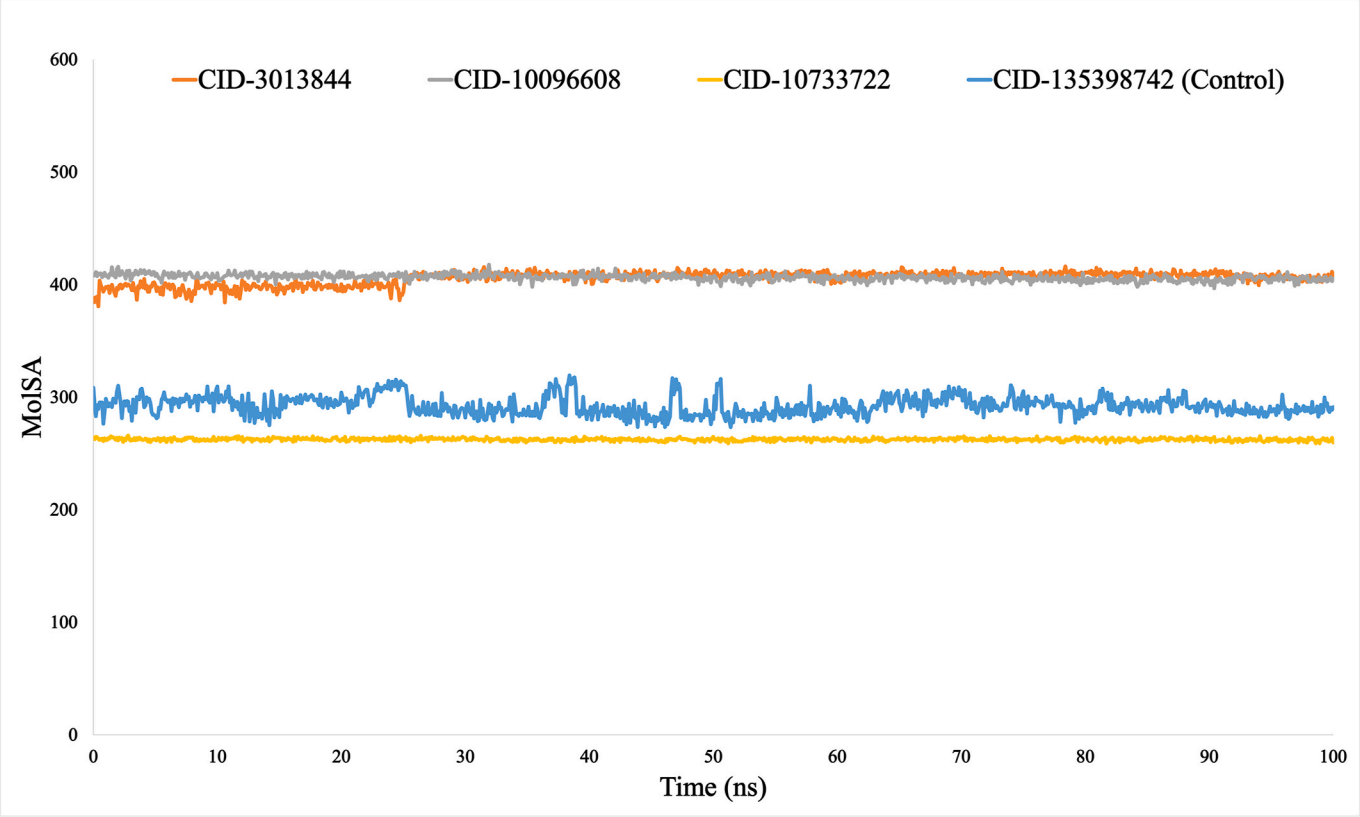

Fig. 9. The molecular surface area (MolSA) of the protein-ligand interaction compounds was calculated from the simulation interaction data at 100 ns. The selected compounds, capituloside (CID: 3013844), pilosidine (CID: 10096608), curcapital (CID: 10733722), and valacyclovir (CID: 135398742) as control, are represented by red, violet, yellow, and blue colours, respectively, in complex with the protein. (For interpretation of the references to colour in this figure legend, the reader is referred to the Web version of this article.)

thymidine kinase proteins reveal that pilosidine exhibits the highest docking score, showcasing numerous hydrogen bond interactions with amino acids such as Gln90, Thr26, and Arg54, in addition to significant hydrophobic interactions. Capituloside also demonstrates strong docking, featuring notable interactions with Glu192, Lys25, and Gly22. Although curcapital has a slightly lower docking score compared to pilosidine and capituloside, it maintains valuable hydrogen bonds involving Glu48 and Arg143. Conversely, the control ligand, valacyclovir, presents the lowest docking score, indicating a comparatively weaker binding affinity, which aligns with its role as a reference compound for comparison purposes.

3.5. Post docking data visualization

In this study, the interactions between the target protein and four distinct ligands were analysed using Ligplot + version 2.2 and Biovia Discovery Studio Visualiser 2021. The interaction data for the docked complexes, which primarily involve hydrophobic contacts and hydrogen bonds, are summarized in Table 2 and illustrated in Fig. 4.

The interaction between capituloside and thymidine kinase protein involved ten hydrophobic contacts (Tyr21, Leu50, Ile62, Thr26, Glu48, Ala134, Phe93, Phe139, Ser135, and Trp53) and four hydrogen bonds (Glu192 – 2.73 Å, Lys25 – 3.28 Å, Gly22 – 2.87 Å, Arg130 – 2.91 Å, Tyr66 – 2.80 Å).

Similarly, the interaction between pilosidine and thymidine kinase protein included ten hydrophobic contacts (Tyr66, Ser135, Ile65, Ile62, Glu192, Tyr21, Leu50, Glu48, Phe139, Phe93) and four hydrogen bonds (Gln90 – 2.76 Å, Gln90 – 2.94 Å, Thr26 – 2.64 Å, Arg54 – 2.94 Å).

Lastly, the interactions of curcapital and valacyclovir with thymidine kinase protein featured three hydrogen bonds (Glu48 – 2.58 Å, Arg143 – 2.70 Å, Gln90 – 2.53 Å) and eight hydrophobic contacts (Arg130, His97, Ala134, Trp53, Phe93, Phe139, Ile65, Tyr66, and Tyr21) and eleven hydrophobic contacts (Glu48, Ile62, Trp53, Phe93, Tyr21, Phe139, Gln90, Ser135, Ala134, Arg130, and Lys25) and three hydrogen bonds (Thr26 – 2.80 Å, Thr26 – 3.19 Å, Gly22 – 2.95 Å), respectively (Fig. 4).

3.6. Computational analysis of physiological and ADMET properties

Computational methods for evaluating physiological and ADMET properties (Absorption, Distribution, Metabolism, Excretion, and Toxicity) properties offer a rapid, efficient, and precise approach (Šestić et al., 2023). In our study, we evaluated the physiological and ADMET characteristics of four compounds—capituloside, pilosidine, curcapital, and valacyclovir as a control using SwissADME and pkCSM tools. The results are presented in Table 3.

The physicochemical and pharmacological properties of the ligands for thymidine kinase proteins reveal significant insights into their potential efficacy and drug-likeness. Capituloside and Pilosidine both have molecular weights of 478.45 g/mol, with 11 hydrogen acceptors (HAc), 7 hydrogen donors (HD), and 6 rotatable bonds (NRB). They both exhibit moderate synthetic accessibility scores (SA: 186.37), are classified as drug-like (DL), and have low toxicities (LD50: 2.665). Curcapital has a lower molecular weight (310.26 g/mol), with 6 HAc, 4 HD, and 1 NRB. It has a favourable synthetic accessibility score (SA: 111.13), is drug-like, and shows lower toxicity (LD50: 2.491) compared to Valacyclovir. Valacyclovir serves as a control with a molecular weight of 324.34 g/mol, 7 HAc, 3 HD, and 8 NRB, showing higher toxicity (LD50: 2.282) but favourable synthetic accessibility (SA: 151.14). These data suggest that capituloside, pilosidine, and curcapital exhibit promising physicochemical properties and pharmacological profiles, warranting

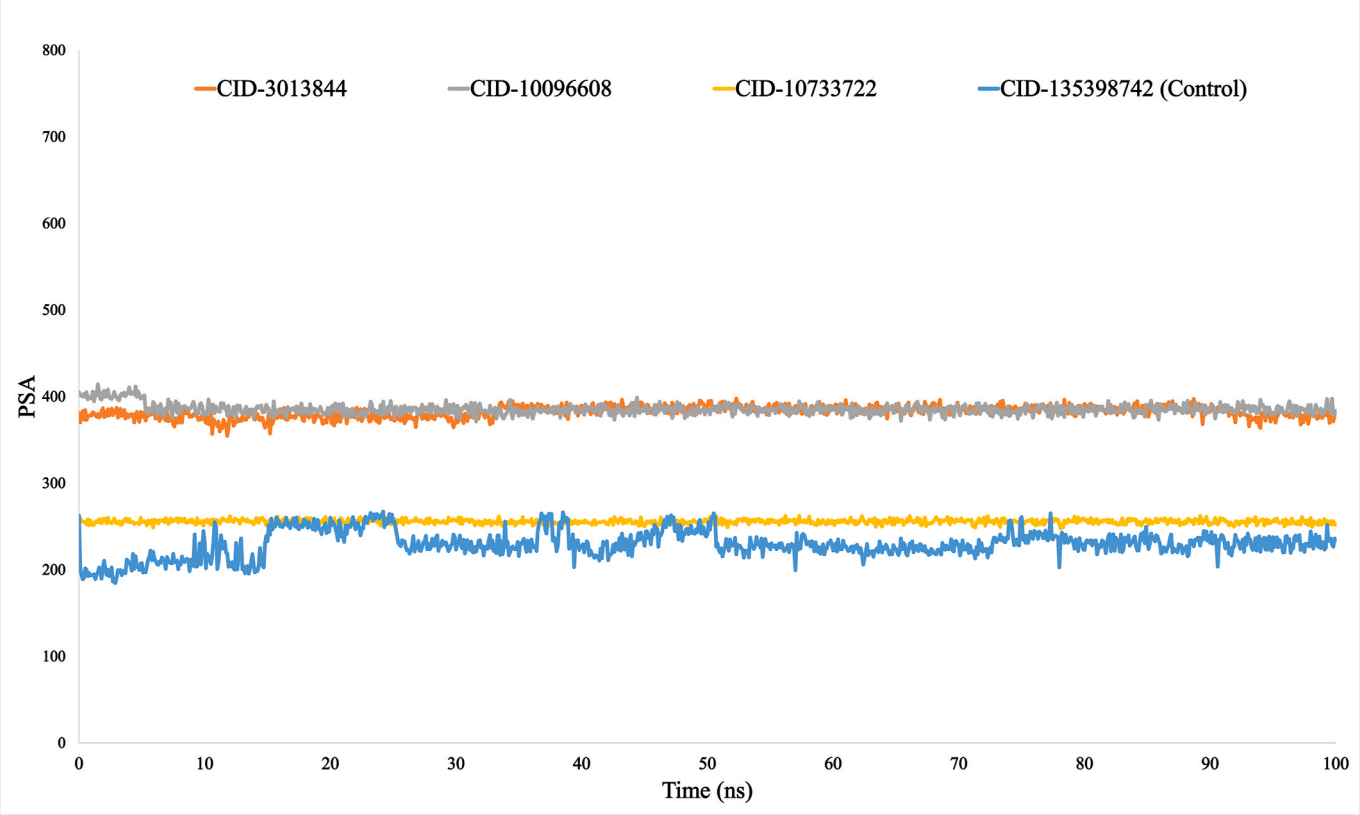

Fig. 10. The polar surface area (PSA) of the protein-ligand interaction compounds was calculated from the 100 ns simulation data. The selected compounds capituloside (CID: 3013844), pilosidine (CID: 10096608), curcapital (CID: 10733722), and valacyclovir (CID: 135398742) as control, are represented by red, violet, yellow, and blue colours, respectively, in complex with the protein. (For interpretation of the references to colour in this figure legend, the reader is referred to the Web version of this article.)

further investigation for their potential as antiviral agents. Other physicochemical parameters, such as the number of hydrogen bond acceptors, hydrogen bond donors, rotatable bonds, AMES toxicity, and maximum tolerable dose, were also within acceptable ranges. In particular, all compounds exhibited drug-like properties and adhered to the Lipinski rule of four. The comprehensive physicochemical and pharmacological characteristics of these compounds are detailed in Table 3.

Additionally, the Supplementary Table 1S demonstrates how different compounds interact with cytochrome P450 (CYP) enzymes, which are essential for drug metabolism. Capituloside and pilosidine show no substrate or inhibitory effects on any tested CYP enzymes (CYP2D6, CYP3A4, CYP1A2, CYP2C19, CYP2C9), indicating a neutral interaction profile. On the other hand, curcapital is a substrate for CYP2D6 and CYP3A4 and inhibits CYP1A2, CYP2C19, and CYP2C9, though it does not affect CYP2D6 or CYP3A4. As a control, valacyclovir shows no interaction with any tested CYP enzymes, providing a reference point. These findings suggest that curcapital may influence its metabolism and potential drug-drug interactions due to its significant enzyme interactions, whereas capituloside and pilosidine are likely to have fewer metabolic complications.

3.7. Molecular dynamic (MD) simulation and Prime MM-GBSA analysis

Molecular dynamics (MD) simulation is a crucial technique in computer-aided drug discovery that is used to understand the stability and intermolecular interactions of a protein-ligand complex in real time. This method also helps to determine the conformational changes of a complex system when exposed to an artificial environment. In this study, a 100 ns MD simulation of the protein in association with the specific ligand was conducted to better understand the conformational changes of the protein-ligand complex. The analysis of intermolecular behaviour was initially performed using terminal snapshots from the 100 ns MD simulation trajectories.

3.7.1. RMSD analysis

The average change in the RMSD of the protein-ligand interaction is considered acceptable within a range of 1–4 Å. If the RMSD value exceeds 1–4 Å, it indicates that the protein structure has undergone a significant conformational change. To determine the conformational changes of the target protein in complex with the four ligand compounds—capituloside, pilosidine, curcapital, and valacyclovir as a control—a 100-ns MD simulation was performed and the corresponding RMSD values were calculated.

For the ligand compound capituloside, the average RMSD ranged between 1 and 2 Å, indicating minimal fluctuations. Similarly, the other ligand compounds—pilosidine, curcapital, and valacyclovir as a control—also exhibited RMSD values within the range of 1.0–2.2 Å. These values showed very little fluctuation, which is below the acceptable threshold, suggesting the conformational stability of the protein-ligand complex structures as depicted in Fig. 5.

3.7.2. RMSF analysis

The RMSF values can help characterise and determine the local changes within the protein chain when selected ligand compounds interact with specific residues. Therefore, the RMSF values for the compounds Capituloside (CID: 3013844), Pilosidine (CID: 10096608), Curcapital (CID: 10733722), and Valacyclovir (CID: 135398742) as a control were calculated to analyses the alterations in protein structural flexibility caused by the binding of these ligands to specific residues.

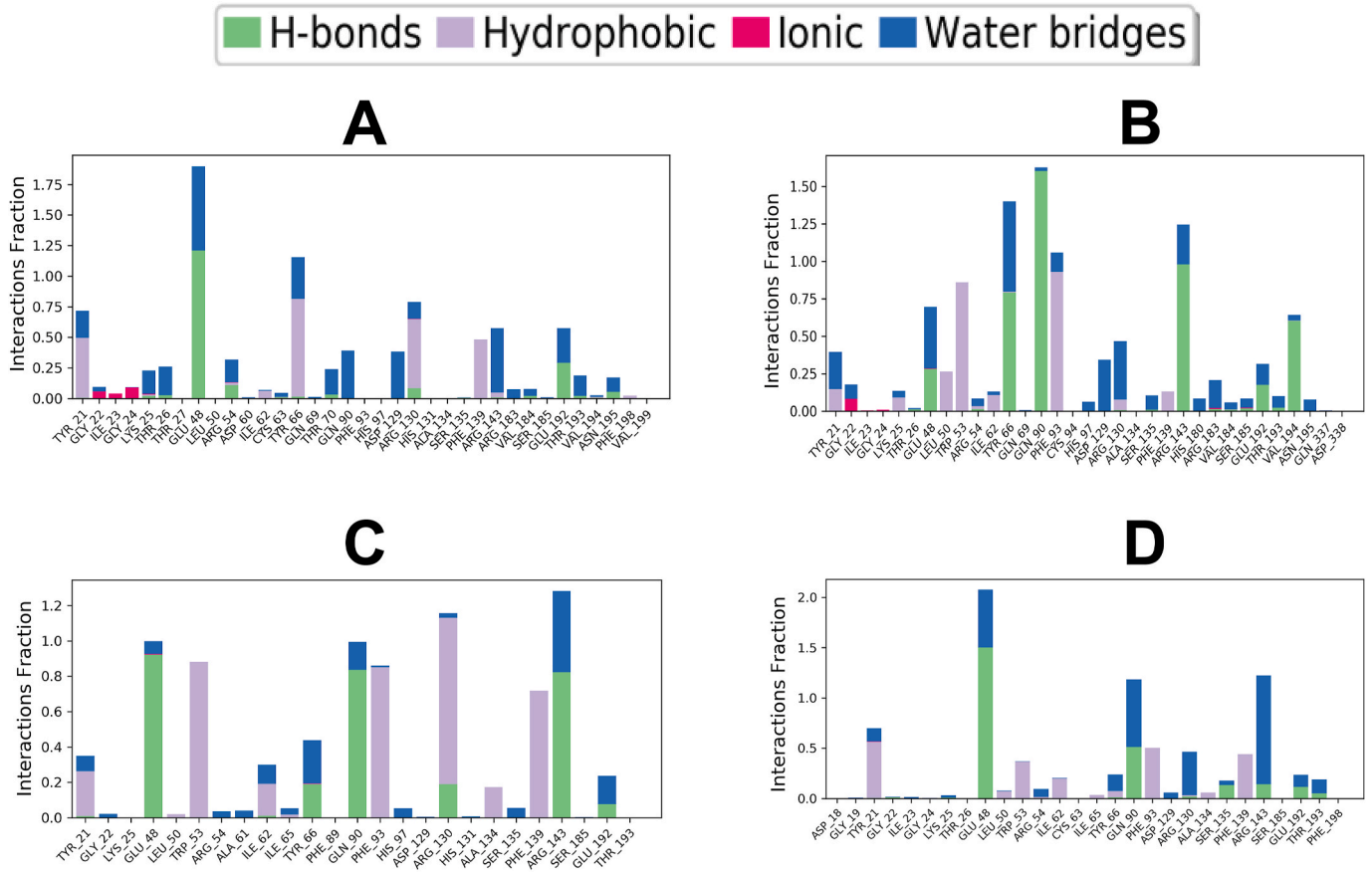

Fig. 11. The stacked bar charts illustrate the interactions between the protein and the selected ligands observed during the 100 ns simulation. This section details the interactions of the four ligand compounds—Capituloside (CID: 3013844), Pilosidine (CID: 10096608), Curcapital (CID: 10733722), and Valacyclovir (CID: 135398742) as a control—in complex with the protein. Figures A–D correspond to Capituloside (CID: 3013844), Pilosidine (CID: 10096608), Curcapital (CID: 10733722), and Valacyclovir (CID: 135398742) (Control), respectively.

These changes are illustrated in Fig. 6.

It was found that the most rigid secondary structural elements, such as alpha-helices and beta-strands, exhibited minimal fluctuations within the residue range of 175–190 amino acids. Because of the presence of the N- and C-terminal domains, the majority of fluctuations were observed at the beginning and end of the protein. Consequently, it can be concluded that in the simulation environment, the displacement of individual atoms has a low probability of fluctuation for the two ligand compounds studied.

3.7.3. *Rg analysis*

The Rg of a protein-ligand interaction system characterises the distribution of its atoms around its axis. When predicting the structural functionality of a macromolecule, calculating Rg is crucial, as it indicates changes in the compactness of the complex over time.

As a result, the stability of capituloside, pilosidine, curcapital, and valacyclovir (Control) was investigated in terms of Rg over a simulation duration of 100 ns, as demonstrated in Fig. 7. The average Rg values for these compounds ranged between 3.6 and 5.0, indicating that the protein's binding site does not undergo significant structural alterations upon binding of the selected ligand compounds. However, in the Rg graph, pilosidine showed more fluctuation compared to the other selected bioactive compounds.

3.7.4. *SASA analysis*

The structural conformation and functions of biological macromolecules are influenced by the solvent accessible surface area (SASA). Typically, amino acid residues on the surface of a protein act as active sites or interact with other molecules and ligands. This interaction improves our understanding of the solvent-like behaviors of a molecule (whether hydrophilic or hydrophobic) and the components of protein-ligand interactions.

The SASA values for the protein complexes with the four ligand compounds were determined and plotted in Fig. 8. Average SASA values for capituloside, pilosidine, curcapital, and valacyclovir (control) ranged from 0 to 360 $Å^2$. This indicates a high level of exposure of amino acid residues to selected compounds in complex simulation systems (Fig. 8).

3.7.5. *MolSA analysis*

The molecular surface area (MolSA) is equivalent to the van der Waals surface area, calculated using a 1.4 probe radius. In our in-silico study, the four compounds capituloside, pilosidine, curcapital, and valacyclovir as a control, exhibited standard van der Waals surface areas, as shown in Fig. 9.

3.7.6. *PSA analysis*

Additionally, the polar surface area (PSA) of a molecule is contributed solely by oxygen and nitrogen atoms. In this study, all compounds exhibited strong PSA values when interacting with the targeted protein (Fig. 10).

3.7.7. *Intramolecular bonds analysis*

Through the simulation interaction diagram (SID), the complex configuration of a protein with the specified ligands and their intermolecular interactions was analysed over a simulation period of 100 ns.

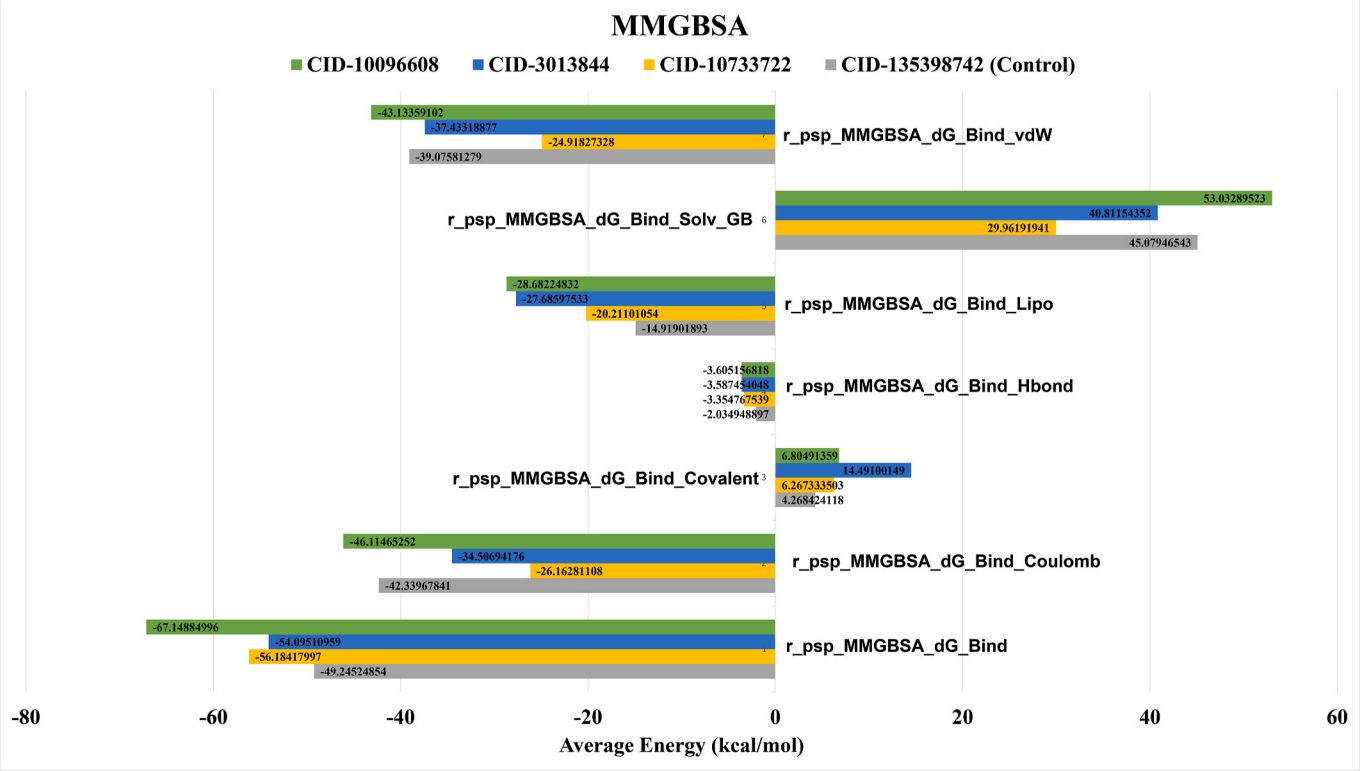

Fig. 12. Post docking binding free energy (MM-GBSA) calculation of the selected phytocompounds with the thymidine kinase protein. Pilosidine (CID: 10096608), Capituloside (CID: 3013844), Curcapital (CID: 10733722), and Valacyclovir (CID: 135398742).

The interactions between the protein and the selected ligand compounds were characterised by several types of bonds, including hydrogen bonds, noncovalent (hydrophobic) bonds, ionic bonds, and water bridge bonds. Fig. 11 illustrates these interactions for the four ligand compounds: capituloside, pilosidine, curcapital, and valacyclovir as control.

Throughout the 100 ns simulation, it was observed that all compounds formed multiple connections via hydrogen, hydrophobic, ionic, and water bridge bonds. These interactions were maintained until the end of the simulation, contributing to the formation of a stable binding with the target protein.

3.7.8. Prime MM-GBSA analysis

MM-GBSA calculations of the chosen compounds—pilosidine, capituloside, curcapital, and valacyclovir (control)—generated negative MM-GBSA ΔG bind (NS) scores of −67.15, −54.09, −56.18, and −49.24 kcal/mol, respectively. Furthermore, the analysis of binding free energy values for each docked complex of thymidine kinase-ligands revealed the performance of ΔG Bind vdW (van der Waals interaction energy), ΔG Bind lipo (Lipophilicity energy), and ΔG Bind Coulomb (Coulomb energy) in complex stability. These results demonstrate the strong binding of target compounds such as pilosidine, capituloside, and curcapital in contrast to the control drug valacyclovir with thymidine kinase (Fig. 12).

4. Discussion

Since ancient times, medicinal plants have been used to treat a variety of infectious diseases. This enduring practice involves the development of drugs through experimentation with different medicinal plants (Siddique et al., 2021). Beyond experimental studies, molecular docking offers insights into potential molecular mechanisms by predicting ligand-target interactions, thereby clarifying how compounds exert their pharmacological effects. This highlights the importance of combining traditional medicinal knowledge with modern computational techniques to discover new biomedicines against varicella-zoster virus thymidine kinase, which plays a vital role in viral DNA replication (Kwofie et al., 2022).

In the present study, 24 *Molineria capitulata* phytochemicals were virtually screened against the thymidine kinase protein, a varicella-zoster virus protein. Four of these twenty-four compounds exhibited binding affinities of −10 kcal/mol or less toward the protein targets, indicating excellent binding. The phytochemical compounds that bound to the active site of the varicella-zoster virus proteins revealed molecular mechanisms of interaction, suggesting that these compounds could inhibit virus activities and prevent them from infecting host cells (Sauerbrei, 2016).

According to molecular docking analysis, pilosidine exhibited the strongest binding affinity to the thymidine kinase protein at −12.471 kcal/mol, indicating a highly effective potential to inhibit viral activities. Capituloside showed the second highest binding affinity at −12.213 kcal/mol, also demonstrating significant promise.

Furthermore, curcapital showed strong binding affinities of −11.360, compared to the control drug valacyclovir, which had a binding affinity of −5.807 kcal/mol. These three compounds, along with the control drug, all had binding affinities of −10 kcal/mol or less toward the targeted proteins, as shown in Table 2. The results of this study suggest that capituloside, pilosidine, and curcapital are the most likely bioactive components that exert antiviral activities against the varicella-zoster virus. Additional validation through in-vitro and in-vivo studies is essential to support computational findings and explore these compounds for potential drug development (Musa et al., 2024).

However, during clinical trials, the pharmacokinetic properties and toxicity often pose significant challenges in the development of drug candidates. Therefore, it is crucial to identify candidates that are drug-like and have comprehensive information about their absorption, distribution, metabolism, excretion, and toxicity (ADMET) to initiate the drug discovery process. The structure of a compound determines its physical and chemical properties, as well as its ADMET profile. In this

study, various servers were used to analyses several ADME descriptors, including physicochemical properties, pharmacokinetics, and drug likeness. According to the Lipinski rule of four, the four selected compounds can be considered druglike. According to Lipinski's rule of four, an orally administered compound must meet the following criteria: molecular weight less than 500 amu, lipophilicity (log P) value of 5 or less, no more than 5 hydrogen bond acceptors, and no more than 10 hydrogen bond donors. Compounds that violate these rules typically have limited bioavailability (Kwofie et al., 2022). The ADMET analysis offers valuable insights, yet a deeper discussion on metabolic stability and potential off-target effects is needed (Akash et al., 2022; Matin et al., 2021).

The analysis of biomolecular interactions and the interface between protein structure and activity can significantly aid in drug development. This is achieved through performance data from dynamic trajectory analysis, known as molecular dynamics simulation (MDS). In our study, we used the Schrödinger package software (Desmond Application) to run a 100-ns MDS with selected physiological and physicochemical parameters. This simulation trajectory was utilised to analyse various metrics, including RMSD, RMSF, Rg, PSA, hydrogen bond number, and SASA.

The RMSD of the alpha carbon and backbone of the selected thymidine kinase protein model was used to evaluate the stability of the protein structure and identify conformational changes; lower RMSD values indicate more stable compounds. In our study, the RMSD values of protein-ligand interactions were within an appropriate range, with average mean values of 1.6 Å (ranging from approximately 1.0 Å to a maximum of 2.2 Å). This suggests a favourable docking position and no disruption of the protein-ligand structure (Fig. 5). The RMSF allows for the quantification of average protein fluctuations from a reference location, with RMSF plots demonstrating fluctuations at the residue level. The RMSF of the C-alpha atoms is illustrated in Fig. 6.

Rg measures the distance between the centre of mass and the end portion of a protein, quantifying the compactness of the molecule and providing information on its folding properties. A higher Rg value indicates slack packing, whereas a lower Rg value signifies compact packing. As shown in Fig. 7, the Rg values for all compounds with the protein demonstrated standard compactness.

The SASA of the protein-ligand complexes was determined using simulation trajectories to assess the dimensional changes of the drug-like molecules. Higher SASA values often indicate an unstable structure with hydrophobic amino acid residues exposed to water molecules. According to the SASA results of the molecular dynamics simulation trajectory, capituloside exhibited higher SASA values compared to the other compounds (Fig. 8). In the MolSA and PSA validation graphs, all ligand compounds showed greater potential than the control drug Acyclovir (Figs. 8 and 9).

Conformational stability was assessed by counting the total number of intermolecular bonds formed between the selected protein macromolecule and its ligand compounds. As shown in Fig. 11, the compounds capituloside, pilosidine, curcapital, and control valacyclovir developed a significant number of intramolecular bonds with the targeted proteins.

The MM-GBSA study of thymidine kinase ligand-receptor complexes revealed favourable binding free energies (ΔG bind) for several compounds. Pilosidine exhibited a ΔG bind of −67.15 kcal/mol, capituloside −54.09 kcal/mol, curcapital −56.18 kcal/mol, and the control, valacyclovir, −49.24 kcal/mol. Notably, pilosidine and curcapital showed significant van der Waals and Coulombic contributions, with higher negative ΔG bind values indicating stronger binding interactions. These findings suggest that pilosidine and curcapital may be more potent thymidine kinase inhibitors than the control compound. Consistent with previous research on electrostatic and hydrophobic interactions, these results highlight the potential of these substances as effective inhibitors. However, further research, including experimental validation and molecular dynamics simulations, is required to verify their therapeutic potential (Fatima et al., 2023; Bhattacharya et al., 2023).

Additionally. pilosidine, also known as curcapicycloside, is a norlignan glucoside that exhibits antibacterial activity against *Escherichia coli* (Zulfiqar et al., 2020). Norlignans, in general, are known for their anti-inflammatory, antiviral, antibacterial, and antifungal activities (Frezza et al., 2020). However, there are no reports of antimicrobial activity for capituloside and curcapital. Overall, the methanolic extract of *Molineria capitulata* leaves has shown significant antioxidant, cytotoxic, thrombolytic, anti-inflammatory, and analgesic activities (Shovo et al., 2021).

5. Future perspective

In our study, capituloside, curcapital, and pilosidine demonstrate strong binding affinity with the crystal structure of varicella-zostervirus thymidine kinase in complex with BVDU-MP and ADP, indicating their potential as drug candidates against chickenpox. The in-silico analysis emphasizes the need for further in-vivo and in-vitro studies to fully elucidate their mechanisms of action, bioavailability, pharmacokinetics, potential toxicity, and therapeutic antiviral potential. Additionally, clinical research is essential to refine and standardize the phytomedicine formulations used by the Musahar tribal healer for treating chickenpox. Investigating the synergistic mechanisms of the polyherbal formulation is crucial to prevent any potential negative interactions.

6. Conclusion

Molineria capitulata, or palm grass, is renowned for its significant ethnomedicinal properties against infections. This plant contains essential phytochemicals and has demonstrated antimicrobial efficacy in various studies. Our in-silico evaluation, which included molecular docking, molecular dynamics simulation, ADMET, and MM-GBSA analysis, revealed that the compounds capituloside, curcapital, and pilosidine from *M. capitulata* exhibit strong binding affinity with the varicella-zoster virus thymidine kinase in complex with BVDU-MP and ADP. These phytochemicals also have favourable pharmacokinetic profiles and are easily synthesized, as indicated by their synthetic accessibility scores. The promising in-silico results for capituloside, curcapital, and pilosidine suggest the need for further in-vitro and in-vivo studies to evaluate the antiviral efficacy of *M. capitulata*. Traditionally used in polyherbal medicine by Musahar tribal healers in Bangladesh to treat chickenpox, this plant's potential is further highlighted by combining ethnomedicinal knowledge with modern computational techniques. In conclusion, integrating traditional medicinal practices with contemporary in-silico analysis emphasizes the potential of *Molineria capitulata* in developing new antiviral therapies. Continued research and validation through in-vitro and in-vivo studies are essential to fully harness the therapeutic potential of its phytocompounds, particularly capituloside, curcapital, and pilosidine.

CRediT authorship contribution statement

Md. Nur Kabidul Azam: Writing - review & editing, Writing - original draft, Validation, Resources, Methodology, Investigation. **Md Nasir Ahmed:** Writing – review & editing, Writing – original draft, Visualization, Methodology, Conceptualization. **Partha Biswas:** Software, Resources, Formal analysis. **Amia Kandker:** Investigation. **Md. Mohaimenul Islam Tareq:** Software, Investigation. **Labib Shahriar Siam:** Software. **Md. Nazmul Hasan:** Validation, Supervision, Resources.

Funding

This study has received no external or internal funding.

Declaration of competing interest

The authors declare that they have no known competing financial interests or personal relationships that could have appeared to influence the work reported in this paper.

Acknowledgement

The authors are grateful to the healers of the Musahar community residing in the Biral subdistrict of Dinajpur district, Bangladesh.

Appendix A. Supplementary data

Supplementary data to this article can be found online at https://doi.org/10.1016/j.amolm.2025.100074.

References

Ahmed, M.N., Hughes, K., 2022. Role of ethno-phytomedicine knowledge in healthcare of COVID-19: advances in traditional phytomedicine perspective. Beni-Suef Univ J Basic Appl Sci 11, 96. https://doi.org/10.1186/s43088-022-00277-1.

Akash, S., Kumer, A., Chandro, A., Chakma, U., Matin, M.M., 2022. Quantum calculation, docking, ADMET and molecular dynamics of ketal and non-ketal forms of D-glucofuranose against bacteria, black & white fungus, and triple-negative breast cancer. Biointerface Res Appl Chem 13, 374. https://doi.org/10.33263/BRIAC134.374.

Arvin, A.M., 1996. Varicella-zoster virus. Clin. Microbiol. Rev. 9, 361–381. https://doi.org/10.1128/CMR.9.3.361.

Ayob, M.A., Nutman, A., Lee, L.H., Alias, A., Khamis, S., Boon, N.E.F.R.H., et al., 2016. Indigenous plants and tuber as alternative food sources for Temiar communities during flood situations. Adv. Environ. Biol. 10, 93–100. https://www.aensiweb.net/AENSIWEB/aeb/aeb/2016/January/93-100.pdf.

Banerjee, P., Eckert, A.O., Schrey, A.K., Preissner, R., 2018. ProTox-II: a webserver for the prediction of toxicity of chemicals. Nucleic Acids Res. 46, W257–W263. https://doi.org/10.1093/nar/gky318.

Bhattacharya, P., Abualnaja, K.M., Javed, S.J., 2023. Theoretical studies, spectroscopic investigation, molecular docking, molecular dynamics and MMGBSA calculations with 2-hydrazinoquinoline. J. Mol. Struct. 1274, 134482. https://doi.org/10.1016/j.molstruc.2022.134482.

Bitew, M., Desalegn, T., Demissie, T.B., Belayneh, A., Endale, M., Eswaramoorthy, R., 2021. Pharmacokinetics and drug-likeness of antidiabetic flavonoids: molecular docking and DFT study. PLoS One 16, e0260853. https://doi.org/10.1371/journal.pone.0260853.

Briliani, M., Perdana, M.C., Perwirasari, I.Y., Setiyaningrum, I.F., Giyarsih, S.R., Haryono, E., 2018. Potency of *Curculigo capitulata* and *Curculigo latifolia* fruit based on nutrient content (a case for preservation need in kebonharjo). Biotropica 2, 67–72. https://doi.org/10.29080/biotropic.2018.2.2.67-72.

Changkija, S., 1999. Folk medicinal plants of the nagas in India. Asian Folk Stud. 58, 205. https://doi.org/10.2307/1178894.

Daina, A., Michielin, O., Zoete, V., 2017. SwissADME: a free web tool to evaluate pharmacokinetics, drug-likeness and medicinal chemistry friendliness of small molecules. Sci. Rep. 7, 42717. https://doi.org/10.1038/srep42717.

David, T., Adelakun, N., Omotuyi, O., Metibemu, D., Ekun, O., Eniafe, G., Inyang, O., Adewumi, B., Enejoh, O., Owolabi, R., Oribamise, E.I., 2018. Molecular docking analysis of phyto-constituents from *Cannabis sativa* with pfDHFR. Bioinformation 14, 574. https://doi.org/10.6026/97320630014574.

De Castro Barbosa, E., Alves, T.M.A., Kohlhoff, M., Jangola, S.T.G., Pires, D.E.V., Figueiredo, A.C.C., Alves, É.A.R., Calzavara-Silva, C.E., Sobral, M., Kroon, E.G., Rosa, L.H., Zani, C.L., De Oliveira, J.G., 2022. Searching for plant-derived antivirals against dengue virus and Zika virus. Virol. J. 19, 31. https://doi.org/10.1186/s12985-022-01751-z.

Dembitsky, V.M., 2005. Astonishing diversity of natural surfactants: 5. Biologically active glycosides of aromatic metabolites. Lipids 40, 869–900. https://doi.org/10.1007/s11745-005-1449-2.

Depledge, D.P., Sadaoka, T., Ouwendijk, W.J.D., 2018. Molecular aspects of varicella-zoster virus latency. Viruses 10, 349. https://doi.org/10.3390/v10070349.

Eshleman, E., Shahzad, A., Cohrs, R.J., 2011. Varicella zoster virus latency. Future Virol. 6, 341–355. https://doi.org/10.2217/fvl.10.90.

Fatima, A., Arora, H., Bhattacharya, P., Siddiqui, N., Abualnaja, K.M., Garg, P., Javed, S. J., 2023. DFT, molecular docking, molecular dynamics simulation, MMGBSA calculation and hirshfeld surface analysis of 5-sulfosalicylic acid. J. Mol. Struct. 1273, 134242. https://doi.org/10.1016/j.molstruc.2022.134242.

Fitzgerald, M., Heinrich, M., Booker, A., 2020. Medicinal plant analysis: a historical and regional discussion of emergent complex techniques. Front. Pharmacol. 10, 1480. https://doi.org/10.3389/fphar.2019.01480.

Freer, G., Pistello, M., 2018. Varicella-zoster virus infection: natural history, clinical manifestations, immunity and current and future vaccination strategies. New Microbiol. 41, 95–105. https://www.newmicrobiologica.org/PUB/allegati_pdf/2018/2/95.pdf.

Frezza, C., Venditti, A., Toniolo, C., De Vita, D., Franceschin, M., Ventrone, A., Tomassini, L., Foddai, S., Guiso, M., Nicoletti, M., Serafini, M., Bianco, A., 2020. Norlignans: occurrence in plants and biological activities—a review. Molecules 25, 197. https://doi.org/10.3390/molecules25010197.

Gershon, A.A., 2017. Is chickenpox so bad, what do we know about immunity to varicella zoster virus, and what does it tell us about the future? J. Infect. 74, S27–S33. https://doi.org/10.1016/S0163-4453(17)30188-3.

Gershon, A.A., Breuer, J., Cohen, J.I., Cohrs, R.J., Gershon, M.D., Gilden, D., Grose, C., Hambleton, S., Kennedy, P.G.E., Oxman, M.N., Seward, J.F., Yamanishi, K., 2015. Varicella zoster virus infection. Nat. Rev. Dis. Primers 1, 15016. https://doi.org/10.1038/nrdp.2015.16.

Islam, M., Parvez, A., 2013. Dalit Initiatives in Bangladesh, first ed. Nagorik Uddyog & Bangladesh Dalit and Excluded Rights Movement, Dhaka, Bangladesh https://idsn.org/wp-content/uploads/2015/01/Dalit-Initiatives-in-Bangladesg.pdf.

Johnston, R.C., Yao, K., Kaplan, Z., Chelliah, M., Leswing, K., Seekins, S., Watts, S., Calkins, D., Chief Elk, J., Jerome, S.V., Repasky, M.P., Shelley, J.C., 2023. Epik: pK_a and protonation state prediction through machine learning. J. Chem. Theor. Comput. 19 (8), 2380–2388. https://doi.org/10.1021/acs.jctc.3c00044.

Kennedy, P., Mogensen, T., Cohrs, R., 2021. Recent issues in varicella-zoster virus latency. Viruses 13, 2018. https://doi.org/10.3390/v13102018.

Kennedy, P.G.E., Gershon, A.A., 2018. Clinical features of varicella-zoster virus infection. Viruses 10, 609. https://doi.org/10.3390/v10110609.

Kichu, M., Malewska, T., Akter, K., Imchen, I., Harrington, D., Kohen, J., Vemulpad, S.R., Jamie, J.F., 2015. An ethnobotanical study of medicinal plants of Chungtia village, Nagaland, India. J. Ethnopharmacol. 166, 5–17. https://doi.org/10.1016/j.jep.2015.02.053.

Komara, F.A., 2009. Herpes zoster vaccination: benefits and barriers. J. Am. Osteopath. Assoc. 109, S22–S24.

Kwofie, S.K., Annan, D.G., Adinortey, C.A., Boison, D., Kwarko, G.B., Abban, R.A., Adinortey, M.B., 2022. Identification of novel potential inhibitors of varicella-zoster virus thymidine kinase from ethnopharmacologic relevant plants through an *in-silico* approach. J. Biomol. Struct. Dyn. 40, 12932–12947. https://doi.org/10.1080/07391102.2021.1977700.

Li, S., Zhang, Y., Guo, Y., Yang, L., Wang, Y., 2020. Monpa, memory, and change: an ethnobotanical study of plant use in Mèdog County, South-east Tibet, China. J. Ethnobiol. Ethnomed. 16, 5. https://doi.org/10.1186/s13002-020-0355-7.

Matin, M.M., Islam, N., Bhattacharjee, S.C., 2021. Regioselective synthesis of some rhamnopyranoside esters for PASS predication, and ADMET studies. Journal of the Turkish Chemical Society Section A: Chemistry 8, 363–374. https://doi.org/10.18596/jotcsa.829658.

Musa, M.S., Miah, M.S., Munni, Y.A., Patwary, M.A.M., Kazi, M., Matin, M.M., 2024. Synthesis and elucidation of strained galactopyronose esters as selective cyclooxygenase-2 inhibitor: a comprehensive computational approach. RSC Adv. 14, 30469–30481. https://doi.org/10.1039/D4RA03520H.

Nie, Y., Dong, X., He, Y., Yuan, T., Han, T., Rahman, K., Qin, L., Zhang, Q., 2013. Medicinal plants of genus *Curculigo*: traditional uses and a phytochemical and ethnopharmacological review. J. Ethnopharmacol. 147, 547–563. https://doi.org/10.1016/j.jep.2013.03.066.

Owen, L., Laird, K., Shivkumar, M., 2022. Antiviral plant-derived natural products to combat RNA viruses: targets throughout the viral life cycle. Lett. Appl. Microbiol. 75, 476–499. https://doi.org/10.1111/lam.13637.

Ozukum, A., Changkija, S., Tripathi, S.K., 2019. Ethnobotanical studies on the khiamniungan tribe in tuensang district of Nagaland, northeast India: ethnomedicinal plants. Pleione 13, 70. https://doi.org/10.26679/Pleione.13.1.2019.070-081.

Panda, S., Roy, P., Mahanty, D.S., 2016. Inventorization and documentation of herbal black salt preparation by the apatanese (Abo-Tani) of Apatani valley in lower subansiri district of Arunachal Pradesh (India) using 'gonde unio' plant (*Ambrosia artemisiifolia* L.—Asteraceae). World Scientific News 47, 254–266.

Pergam, S.A., Limaye, A.P., 2009. Varicella zoster virus (VZV) in solid organ transplant recipients. Am. J. Transplant. 9, S108–S115. https://doi.org/10.1111/j.1600-6143.2009.02901.x.

Pires, D.E.V., Blundell, T.L., Ascher, D.B., 2015. pkCSM: predicting small-molecule pharmacokinetic and toxicity properties using graph-based signatures. J. Med. Chem. 58, 4066–4072. https://doi.org/10.1021/acs.jmedchem.5b00104.

Salmerón-Manzano, E., Garrido-Cardenas, J.A., Manzano-Agugliaro, F., 2020. Worldwide research trends on medicinal plants. IJERPH 17, 3376. https://doi.org/10.3390/ijerph17103376.

Santoso, E.A., Jumari, Utami, S., 2019. Inventory and biodiversity medicinal plants of Dayak tomun society in Lopus village Lamandau regency central Kalimantan. J. Phys.: Conf. Ser. 1217, 012171. https://doi.org/10.1088/1742-6596/1217/1/012171.

Sauerbrei, A., 2016. Varicella-zoster virus infections – antiviral therapy and diagnosis. GMS Infectious Diseases 4, Doc01. https://doi.org/10.3205/ID000019.

Sauerbrei, A., 2016a. Diagnosis, antiviral therapy, and prophylaxis of varicella-zoster virus infections. Eur. J. Clin. Microbiol. Infect. Dis. 35, 723–734. https://doi.org/10.1007/s10096-016-2605-0.

Šestić, T.Lj, Ajduković, J.J., Marinović, M.A., Petri, E.T., Savić, M.P., 2023. In silico ADMET analysis of the A-, B- and D-modified androstane derivatives with potential anticancer effects. Steroids 189, 109147. https://doi.org/10.1016/j.steroids.2022.109147.

Shovo, M.A.R.B., Tona, M.R., Mouah, J., Islam, F., Chowdhury, M.H.U., Das, T., Paul, A., Ağagündüz, D., Rahman, M.M., Emran, T.B., Capasso, R., Simal-Gandara, J., 2021. Computational and pharmacological studies on the antioxidant, thrombolytic, anti-inflammatory, and analgesic activity of *Molineria capitulata*. Curr. Issues Mol. Biol. 43, 434–456. https://doi.org/10.3390/cimb43020035.

Siddique, H., Pendry, B., Rashid, M.A., Rahman, M.M., 2021. Medicinal plants used to treat infectious diseases in the central part and a northern district of Bangladesh – an

ethnopharmacological perception. J. Herb. Med. 29, 100484. https://doi.org/10.1016/j.hermed.2021.100484.

Srivastava, R., Tripathi, S., Unni, S., Hussain, A., Haque, S., Dasgupta, N., Singh, V., Mishra, B.N., 2021. Silybin B and cianidanol inhibit Mpro and spike protein of SARS-CoV-2: evidence from in silico molecular docking studies. CPD 27, 3476–3489. https://doi.org/10.2174/1381612826666201210122726.

Umaru, I.J., Umaru, H.A., Ahuchaogu, C.E., Usman, M.A., 2020. Phytochemical, characterization and antimicrobial studies of *Molineria capitulata* fruits essential oil against multidrug resistance pathogens. Solid State Technol. 63, 90–107. https://solidstatetechnology.us/index.php/JSST/article/view/701.

Xiong, G., Wu, Z., Yi, J., Fu, L., Yang, Z., Hsieh, C., Yin, M., Zeng, X., Wu, C., Lu, A., Chen, X., Hou, T., Cao, D., 2021. ADMETlab 2.0: an integrated online platform for accurate and comprehensive predictions of ADMET properties. Nucleic Acids Res. 49, W5–W14. https://doi.org/10.1093/nar/gkab255.

Yang, J., Chen, W.-Y., Fu, Y., Yang, T., Luo, X.-D., Wang, Yue-Hu, Wang, Yu-Hua, 2020. Medicinal and edible plants used by the Lhoba people in Medog county, Tibet, China. J. Ethnopharmacol. 249, 112430. https://doi.org/10.1016/j.jep.2019.112430.

Yuan, H., Ma, Q., Ye, L., Piao, G., 2016. The traditional medicine and modern medicine from natural products. Molecules 21, 559. https://doi.org/10.3390/molecules21050559.

Yun, T., Zhang, M., Zhou, D., Jing, T., Zang, X., Qi, D., Chen, Y., Li, K., Zhao, Y., Tang, W., Huang, J., Wang, W., Xie, J., 2021. Anti-foc RT4 activity of a newly isolated Streptomyces sp. 5–10 from a medicinal plant (*Curculigo capitulata*). Front. Microbiol. 11, 610698. https://doi.org/10.3389/fmicb.2020.610698.

Zulfiqar, F., Khan, S.I., Ali, Z., Wang, Y.-H., Ross, S.A., Viljoen, A.M., Khan, I.A., 2020. Norlignan glucosides from *Hypoxis hemerocallidea* and their potential in vitro anti-inflammatory activity via inhibition of iNOS and NF-κB. Phytochemistry 172, 112273. https://doi.org/10.1016/j.phytochem.2020.112273.